# A mechanism to prevent transformation of the Whi3 mnemon into a prion.

**Authors**: Yasmin Lau[1], Iuliia Parfenova[2], Juha Saarikangas[3, 4, 5], Yves Barral[2*] and Fabrice Caudron[1*]

**Affiliations**:

1 –School of Biological Sciences, Queen Mary University of London, London, UK.

2 - Institute of Biochemistry, ETH Zürich, Zürich, Switzerland.

3 - Helsinki Institute of Life Science HiLIFE, Helsinki, Finland.

4 - Faculty of Biological and Environmental Sciences, Helsinki, Finland.

5 - Neuroscience Center, University of Helsinki, Helsinki, Finland.

*Correspondence to: f.caudron@qmul.ac.uk or yves.barral@bc.biol.ethz.ch

**Abstract**:

In response to deceptive courtship, budding yeast cells escape pheromone induced cell cycle arrest through coalescence of the G1/S inhibitor Whi3 into a dominant inactive super-assembly. Strikingly, Whi3 super-assemblies remain stable over many cell cycles in the mother cells and are not passed on to the daughter cells. Thereby, Whi3 coalescence encodes memory, conferring to it the property of a mnemon (Whi3$^{mnem}$), a protein which conformational change maintain a trait that is permanent in the mother cell but is not inherited by daughter cells. Mnemons share structural features with prions, which are self-templating protein conformations that are inherited by daughter cells. Yet, how the maintenance and asymmetric inheritance of Whi3$^{mnem}$ are achieved is unknown. Here, we report that Whi3$^{mnem}$ is closely associated with endoplasmic reticulum (ER) membranes and retained in the mother cell by the presence of lateral membrane diffusion barriers at the bud neck. Strikingly, barrier defects made Whi3$^{mnem}$ propagate in a mitotically stable manner, like a prion. Alike Whi3$^{mnem}$, transformation of Whi3 into a prion required its poly-glutamine prion-like domain. Thus, we propose that Whi3$^{mnem}$ is in a self-templating state, lending temporal stability to the memory that it encodes, while its anchorage into the compartmentalized membranes of the ER ensures its confinement in the mother cell and prevents its infectious propagation. These results suggest that confined self-templating super-assembly is a powerful mechanism for the long-term encoding of information.

33 **Introduction**

34 Prions are proteins that can adopt several conformations with at least one of them that is self-
35 templating, lending it a self-perpetuating character. Prion conversion is essential for
36 physiological processes including innate immunity (Hou et al., 2011) and the generation of
37 phenotypic diversity of single celled organisms ranging from bacteria to yeast (Coustou et al.,
38 1997; True and Lindquist, 2000; Yuan and Hochschild, 2017). Beyond physiology, prions were
39 initially discovered to cause Scrapie in sheep and Creutzfeldt-Jakob (Prusiner, 1982). Prion-
40 like behavior may be linked to other diseases including Alzheimer's and Parkinson's diseases
41 (Goedert, 2015), as well as resistance to anti-fungal drugs (Suzuki et al., 2012). What
42 mechanisms control prions and particularly their self-templating activity is still an open
43 question.

44 Prions are common protein elements and several have been identified in the budding yeast
45 *S. cerevisiae* (Wickner et al., 2015) allowing a wealth of research to understand their regulation
46 and function (Harvey et al., 2018). The protein Sup35 can adopt a conformation to form the
47 [*PSI*+] prion, the best characterized to date (Tuite and Cox, 2006). Sup35 is a translation
48 terminator that loses its function in its [*PSI*+] form, resulting in stop codon readthrough and
49 phenotypic diversity (True and Lindquist, 2000). Importantly, Sup35 contains a prion-like
50 domain, defined as rich in Glutamine and Asparagine (Q/N) residues and depleted of charged
51 and hydrophobic residues (Alberti et al., 2009). This domain drives the Sup35 prion state by
52 adopting a self-templating conformation (Serio et al., 2000) and mediating the assembly of
53 Sup35 into amyloid fibrils. Once established, fibrils formed by the Sup35 protein are
54 fragmented into smaller seeds by the protein disaggregase Hsp104 (Narayanan et al., 2006).
55 The self-templating activity of prion seeds converts most of the protein pool to the prion form
56 and the seeds are free to diffuse to the daughter cells. Therefore, prions behave as infectious
57 particles, establishing [*PSI*+] not only in the cell in which it originated but also in all its daughter
58 cells and hence the growing colony. In silico analysis of the yeast proteome has identified
59 around 200 proteins in *S. cerevisiae* containing a potential prion-like domain (Alberti et al.,
60 2009). However, we still do not know if all prion-like domains can adopt self-templating
61 conformations and whether all these proteins function as prions.

62 Whi3 is one of the budding yeast proteins that contains prion-like domains (Alberti et al., 2009;
63 Caudron and Barral, 2013). Whi3 is an mRNA binding protein involved in the timing of the
64 G1/S transition of the cell cycle and the control of cell size in *S. cerevisiae* (Garì et al., 2001).
65 The function of Whi3 that has been studied the most is the regulation of the G1/S transition of
66 the cell cycle through binding and inhibiting the translation of the mRNA that encodes the G1
67 cyclin *CLN3*. This inhibition ensures that entry into S phase is delayed until cells reach a critical

size. The prion-like domains of Whi3 are required for Whi3 to adopt a conformation that releases Whi3's inhibition on *CLN3* mRNA and allows a long-lasting phenotypic switch. Upon exposure to mating pheromone, haploid yeast cells arrest in the G1 phase of the cell cycle and grow towards the source of pheromone. This cytoplasmic projection is termed a shmoo. After prolonged exposure of pheromone without a mating partner in reach, yeast cells become refractory to the pheromone signal and resume their cell cycle (Caudron and Barral, 2013; Moore, 1984). They switch from a shmooing phase to a budding phase. Remarkably, once established, this pheromone refractory state is stable, lending memory to the cell that there is no partner available. As a consequence, these cells keep on budding for the remainder of their life span even in the presence of mating pheromone. Strikingly, daughter cells do not inherit this adaptation and restore their ability to shmoo in response to pheromone upon separation from their mother cell (Caudron and Barral, 2013). Whi3's prion-like domains trigger both escape from pheromone arrest and the memory state by mediating the condensation of Whi3 into super-assemblies.

Therefore, Whi3 share many similarities with prions such as Sup35. The pheromone refractory state is very stable once it has been established, even when pheromone is removed from the medium. The deletion of either prion-like domain of Whi3 results in a late escape from pheromone arrest that is not stably maintained in the mother cells. In other words, cells can switch back and forth to a shmooing and a budding phase in the presence of pheromone. Moreover, when cell extracts are run on a semi-denaturing gel, Whi3 appears to be mostly monomeric in untreated cells and mostly found in large, homo-multimeric assemblies in cell treated with pheromone (Caudron and Barral, 2013). These data point to a possible self-templating activity of Whi3 in cells that are exposed to pheromone.

However, the mode of inheritance of Whi3 super-assemblies is different from the inheritance of prions during cell division (Caudron and Barral, 2013; Tuite, 2016). Indeed, the Whi3 super-assemblies remain in the mother cells at mitosis, ensuring that the memory state is stable in the mother cell and is not propagated to the progeny. On the contrary, prions infect the bud of a dividing yeast cell. Given its role in cellular memory and its behavior being so distinct from prions, Whi3 was called a mnemon ($Whi3^{mnem}$).

While the prion-like domains of $Whi3^{mnem}$ are important for escape from pheromone arrest, we do not know the mechanism of memory stability and if this involves a self-templating activity of $Whi3^{mnem}$. If this is the case, what makes mnemons distinct from prions is unclear. In this work, we wondered whether the confinement of $Whi3^{mnem}$ to the mother cell requires the presence of lateral membrane diffusion barriers. Diffusion barriers are membrane specialized domains that limit the diffusion of membrane associated structures across cellular

appendages (Caudron and Barral, 2009; Saarikangas and Barral, 2011) including the primary cilium (Hu et al., 2010; Kim et al., 2010), dendritic spines (Ewers et al., 2014) and the sperm tail (Toure et al., 2011). In budding yeast, diffusion barriers form at the bud neck in the ER membranes and the nuclear envelope during closed mitosis. Their formation depends on septins, a family of cytoskeletal protein forming filaments (Mostowy and Cossart, 2012) at the bud neck (Luedeke et al., 2005), proteins involved in sphingolipid biosynthesis including the sphinganine C4-hydroxylase Sur2 (Clay et al., 2014) and proteins involved in polarized cell growth such as the actin nucleation promoting factor Bud6 (Graziano et al., 2013, 2011) and the small GTPase Bud1/Rsr1 (Bender and Pringle, 1989). Diffusion barriers in yeast limit the diffusion from the mother cell to the bud of ageing factors, such as nuclear pores, misfolded proteins, age-induced protein deposits and DNA circles (Clay et al., 2014; Denoth-Lippuner et al., 2014; Saarikangas et al., 2017; Shcheprova et al., 2008).

In light of these data, we first asked whether membrane diffusion barriers contribute to Whi3$^{mnem}$ asymmetric behaviour during cell division.

## Results

*Cells lacking diffusion barriers can acquire a novel pheromone refractory state.*

Growth of yeast colonies was monitored on solid medium containing low concentration of pheromone (10nM). Wild type cells grew slowly while cells that hardly escape pheromone arrest (*whi3-ΔpQ,* Caudron and Barral, 2013) grew very poorly (Figure 1A). Both strains grew equally well on a solid medium that does not contain pheromone. On medium containing pheromone, wild type cells initially shmoo and resume cell division after several hours. Their daughter cells behave similarly, first shmooing and then resuming cell division. This slows down the production of daughter cells and explains why wild type cells grow slowly in the presence of pheromone. In contrast, *whi3-ΔpQ* mutant cells keep on shmooing for a very long time before resuming cell division and many cells will not even escape pheromone induced cell cycle arrest. Therefore, *whi3-ΔpQ* mutant cells grow even slower on pheromone containing plates. To test for a role of diffusion barriers in the compartmentalization of the pheromone refractory state, we monitored the growth of several mutant strains with impaired barrier formation. We hypothesized that if diffusion barriers are involved in the confinement of Whi3$^{mnem}$ these mutant strains may grow differently on pheromone. Some of the *bud1Δ*, *bud6Δ* and *sur2Δ* mutants grew as wild type and other much better on pheromone containing plates, even at high pheromone concentration (0.6μM, Fig1A). At such a high concentration of pheromone, cells cannot escape pheromone arrest, suggesting that colonies growing in such

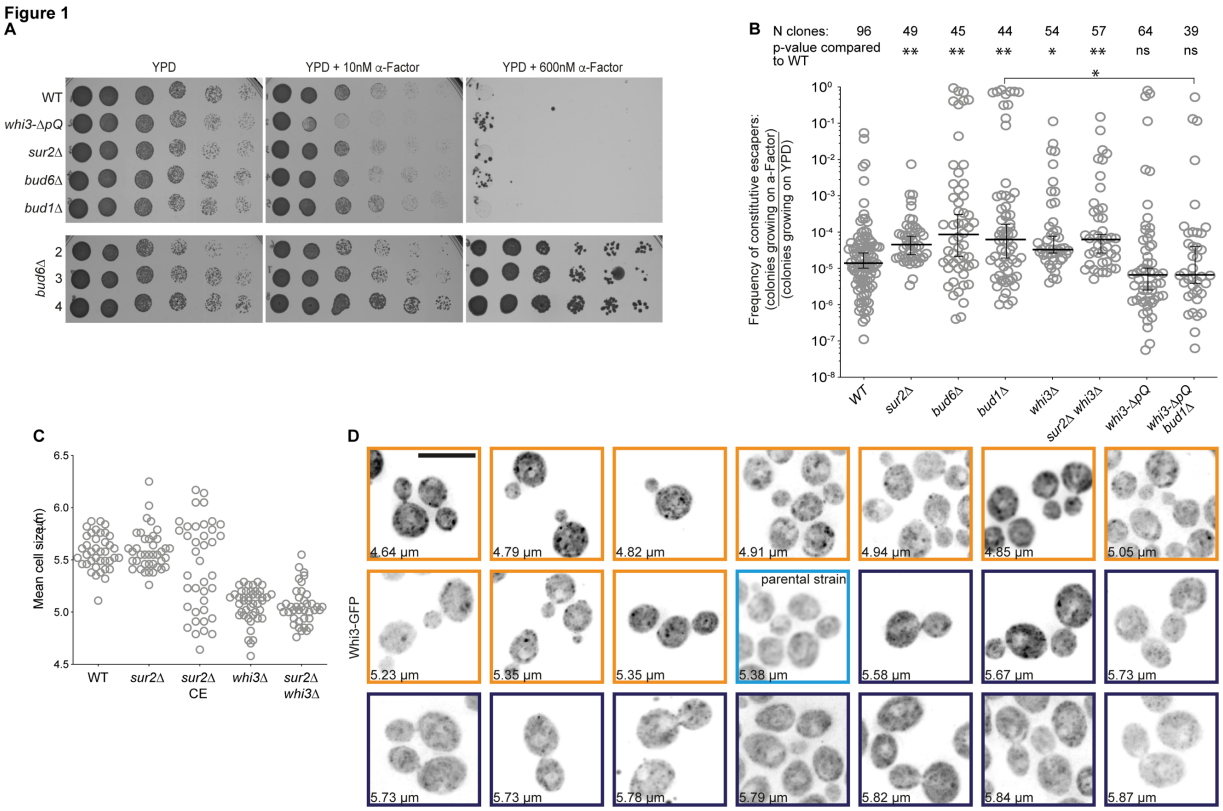


**Figure 1. A novel epigenetic phenotype, constitutive escapers.** (A) Serial 1/10 dilutions of exponentially growing cultures of indicated strains spotted on a YPD solid medium (left) or YPD containing **α**-factor (10nM middle and 600nM right). The bottom panel shows three *bud6*Δ independent clones with high frequency of CE. (B) Frequency of appearance of CEs in the indicated genotypes (median with 95% confidence interval, n>37 clones for each, Dunn's multiple comparisons test was used to determine significance). (C) Cell size distributions of individual clones or CE isolates of indicated strains (n>39 clones for each). (D) Maximal projection images of *sur2*Δ cells expressing Whi3-GFP from 20 CE isolates and the parental strain. Isolates are in order of mean cell size from the smallest (orange frame are smaller than the blue framed parental strain) to the largest (purple are larger than the parental strain). Scale bar = 5µm.

conditions had acquired a strong resistance to pheromone. Colonies growing on high pheromone concentration kept their resistance to pheromone after several rounds of streaking; we termed them constitutive escapers (CE). To measure how frequent CE are, we plated at least 44 independent clones for each mutation obtained from heterozygous diploid on rich media that do not contain pheromone or contain a high pheromone concentration (0.6µM) (Figure 1A-B). Frequency of CE appearance was highly variable between individual clones of wild type strains (between $1.11 \times 10^{-7}$ and $5.3 \times 10^{-2}$) with a median of $1.36 \times 10^{-5}$ cells. Phenotypic mutation rate for sterile mutants was measured in a *bar1*Δ background at $3.07 \times 10^{-6}$/genome/generation (Lang and Murray, 2008). We found that it was also variable in *sur2*Δ clones but the median was significantly increased 3.13 times compared to wild type ($4.26 \times 10^{-5}$, Figure 1B). In *bud6*Δ and *bud1*Δ mutant cells, frequencies again varied extensively between clones and the median frequency was significantly increased 6.07 times ($8.27 \times 10^{-5}$) and 3.51 times ($4.78 \times 10^{-5}$) respectively, compared to wild type. These data suggest that the frequency increase of constitutive escapers is related to the disruption of the diffusion barrier. Moreover, the fact that we measured very variable frequencies and many of them being well above mutation rate suggest that CE are induced by an epigenetic

153 mechanism. Since escape from pheromone arrest involves Whi3$^{mnem}$, we considered the
154 possibility of a prion being the molecular basis of the CE phenotype.
155 Upon microscopic observation of CE, we noticed that some CE isolates seemed to be small
156 cell sized. Therefore, we measured the cell size of several CE. While wild type cells and *sur2*Δ
157 parental strains had comparable cell size (5.6µm, Figure 1C), *sur2*Δ CE displayed isolates
158 which were on the large range or on the small range of cell sizes. Remarkably, the small cell
159 sized were very similar to cells deleted for *WHI3* either in a wild type or in a *sur2*Δ background
160 (Figure 1C). This prompted us to ask whether Whi3 could be a prion in CE isolates and if it
161 was required for the formation of CE. Classically, prion forms of proteins lose the function of
162 the native conformation. Thus, if Whi3 was losing its function in a prion form, we would expect
163 that deleting *WHI3* would result in a CE phenotype. The frequency of CE in *whi3*Δ mutant
164 strains was increased compared to wild type (2.45 times, 3.33 x $10^{-5}$) and further increased in
165 *whi3*Δ *sur2*Δ strains (4.58 times, 6.23 x $10^{-5}$). This result indicate that Whi3 inactivation is not
166 sufficient to make cells refractory to pheromone, although it may contribute to it. We next
167 wondered whether Whi3 was required to maintain the CE phenotype. We supposed that if
168 Whi3 was acting as a dominant negative form in these cells, deleting *WHI3* in *sur2*Δ$^{CE}$ would
169 restore pheromone arrest. We specifically deleted *WHI3* in several *sur2*Δ$^{CE}$ that had a small
170 cell size. This deletion did not restore pheromone arrest (not shown) suggesting that
171 maintenance of the CE phenotype is not dependent on Whi3 or that Whi3 super-assemblies
172 are not the only dominant factor repressing pheromone response in CEs. Altogether, we
173 observe that *whi3*Δ cells are not all CE (most of the cells arrest upon exposure to pheromone)
174 yet deleting *WHI3* seems to favor CE formation. However, Whi3 is not required to maintain
175 the CE phenotype. One interpretation of these results may be that *WHI3* inactivation is one
176 step for cells to become CE. Somehow, the diffusion barrier inhibited the transition to the CE
177 state.

178 To further test whether Whi3 may be in a prion form in CE, we isolated 20 CE from a *sur2*Δ
179 parental strain (*sur2*Δ$^{CE}$) expressing Whi3-GFP from its endogenous locus on plates
180 containing high pheromone concentration and we observed the localization of Whi3-GFP in
181 these cells. In parallel, we obtained cell size measurements of these isolates. In the parental
182 *sur2*Δ strain, Whi3-GFP localized rather diffusely throughout the cytoplasm and to a few
183 granules (Caudron and Barral, 2013; Garì et al., 2001 and Figure 1D). In small cell sized
184 *sur2*Δ$^{CE}$, Whi3 localized diffusely throughout the cytoplasm and to brighter foci that were
185 substantially bigger and more intense than the granules shown by the parental strain. These
186 bright foci were much less frequent in large cell sized CE (Figure 1D). Remarkably, these
187 bright foci localized both to the mother and bud compartments of dividing cells. This is in
188 contrast to Whi3$^{mnem}$ super-assemblies which are formed in the mother cell and do not typically

189 appear in the buds (Caudron and Barral, 2013). Therefore, in small cell sized *sur*2Δ$^{CE}$, Whi3
190 tends to adopt a localization pattern reminiscent to that of the classical yeast prion Sup35, in
191 its [*PSI*+] form (Derdowski et al., 2010). We contemplated the possibility that if Whi3 needs to
192 be in a prion form for cells to become CE, it would require its prion-like domain. To test this
193 hypothesis, we estimated the frequency of CE in *whi3*-Δ*pQ* mutant clones. CE frequency was
194 remarkably lower in these cells than in any other strain we tested (6.25 x $10^{-6}$, 2.18 times
195 smaller than wild type strains, although not significantly different, Figure 1B). Deleting *BUD1*
196 in a *whi3*-Δ*pQ* strain did not increase the frequency of CE much (7.45 x $10^{-6}$, 1.192 times
197 higher than in *BUD1 whi3*-Δ*pQ* mutant strain) and was lower than in *bud1*Δ mutant cells.

198 Altogether, we found that disruption of the diffusion barrier increases the appearance of CE,
199 that many of them are small cell sized and display a localisation of Whi3 to bright foci. The
200 formation of CE is increased when *WHI3* is deleted but decreased in strains that lack the prion-
201 like domain of Whi3. This suggest that Whi3 is indeed in a prion form and that inactivation of
202 Whi3 is a major contribution to the formation of CE. However, since the frequency of CE can
203 be still very high in CE that lack the prion-like domain of Whi3, it is very likely that other factors
204 are involved, possibly novel prions to discover.
205
206 To test whether the molecular events leading to the formation of CE is indeed caused by
207 prions, we tested how growth on high pheromone concentration segregated at meiosis. Prions
208 segregate in a non-Mendelian manner at meiosis and are usually passed on to all of the four
209 meiotic products. Consistent with their extensive resistance to pheromone treatment, crossing
210 the CE to wild type cells was inefficient. However, we could backcross some of them and
211 dissect the obtained tetrads. Meiosis gives rise to 4 spores, 2 of which are *MAT*α and 2 *MAT***a**.
212 Therefore, we expected that out of 4 spores, 2 would always grow on alpha-factor because
213 they are *MAT*α. In wild type cells, the 2 other spores do not grow on alpha-factor (0.6μM,
214 Supplemental Figure1). If in the CE more than 2 spores were growing, it would mean that they
215 had inherited the CE phenotype. If the CE is due a mutation that is unlinked to the *MAT* locus,
216 4/6 of the tetrads should have 3 spores growing on alpha-factor containing medium, 1/6 should
217 contain 4 such spores and the last 1/6 of the tetrads should contain only 2 of them (pattern
218 #1). If it is due to a mutation linked to the *MAT* locus, the fraction of tetrads with 3 and 4 spores
219 growing on alpha-factor containing medium should be increased (pattern #2). In case of a
220 non-mendelian factor propagating through meiosis, all tetrads should contain 4 spores
221 growing on alpha-factor containing medium (pattern #3). Finally, a non-mendelian factor that
222 does not pass meiosis should produce tetrads with always only 2 spores growing on alpha-
223 factor containing medium (pattern #4). We backcrossed 13 independent CE strains and tested
224 the growth of each spore on alpha-factor (0.6μM). For 4 backcrosses, we observed tetrads in

225 which 2, 3 or 4 spores out of 4 were growing on α-factor (Supplemental Figure1). These
226 backcrosses fall in the pattern #1, suggesting the presence of a single 'sterile' mutation
227 segregating independently from the mating type locus. In 4 other backcrosses, the majority of
228 the tetrads contained 2 spores and few 3 spores growing on alpha-factor containing medium,
229 most compatible with the pattern #4. Furthermore, 5 backcrosses followed strictly pattern #4
230 (Supplemental Figure1). Thus, the last 9 backcrosses, which are not compatible with a single
231 mutation, suggests that the CE phenotype is due to non-mendelian factor that is lost during
232 meiosis. To further test if these CE traits are based on a prion-like mechanism, we tested
233 whether they were cured upon inhibiting different prion effectors. We isolated 31 *sur*2Δ$^{CE}$ and
234 passaged them three times on YPD, YPD supplemented with guanidine hydrochloride (3 mM)
235 to inhibit Hsp104 (Ferreira et al., 2001; Tuite et al., 1981) or YPD supplemented with radicicol
236 (10μM) to inhibit Hsp90 (Sharma et al., 1998). In addition, we transformed all 31 *sur*2Δ$^{CE}$ and
237 the parental *sur*2Δ strain with a dominant negative allele of *SSA1* (*SSA1*$^{DN}$, Brown and
238 Lindquist, 2009; Jarosz et al., 2014). In all cases, after 3 passages the 31 *sur*2Δ$^{CE}$ were still
239 able to grow on YPD containing pheromone (0.6μM), while the parental *sur*2Δ strain was not
240 (Supplemental Figure2). However, upon microscopic observation of *sur*2Δ$^{CE1}$, we found that
241 many cells were shmooing and other dividing. This was not the case for other *sur*2Δ$^{CE}$, and it
242 was also not the case for *sur*2Δ$^{CE1}$ passaged on YPD without drugs or with GuHCl or radicicol
243 (Supplemental Figure2). Therefore, the CE phenotype is not cured by either GuHCl, radicicol
244 or passages for many generations on YPD, but one variant was partially cured upon inhibition
245 of the Hsp70 chaperone Ssa1.
246
247 Altogether, our data suggest that the majority of the CE formed in cells lacking a diffusion
248 barrier at the bud neck are due to a non-mendelian factor and that for about at least half of
249 them Whi3 is contributing to their formation by behaving not anymore as a mnemon but as a
250 prion.

251

252 *Endoplasmic reticulum compartmentalization is not required for prion induction and curing.*

253 Because diffusion barriers seem to play a role in the transformation of Whi3 into a prion, we
254 next asked whether diffusion barriers also play a role in prion induction and curing. We
255 specifically focused on the best studied prion in yeast, [*PSI*+]. We previously observed that
256 farnesylation of the Hsp40 co-chaperone Ydj1 was required to lower premature stop codon
257 read-through in the sequence coding for GFP in [*PSI*+] cells (Saarikangas et al., 2017).
258 Strength of codon read-through was linked to the potential collection of prion seeds to ER
259 membranes. We therefore analyzed stop codon readthrough in *sur2*Δ cells. Using flow
260 cytometry, the fluorescence intensity of strains that express a GFP allele containing a
261 premature stop codon was measured (as in Saarikangas et al., 2017). Deletion of *SUR2* did
262 not change the fluorescence intensity of these cells (Figure 2A). We next probed for a role of
263 lateral diffusion barriers in the de novo appearance and curing of [*PSI*+] prions. There was no
264 significant difference (p=0.5204, t-test) in the [*PSI*+] appearance frequencies in wild type and
265 *sur2*Δ strains (Figure 2B). We also analyzed the dynamics of [*PSI*+] curing by Guanidine
266 Hydrochloride (GuHCl, 3 mM) in wild type and *sur2*Δ cells and observed very similar dynamics
267 of curing (Figure 2C). Moreover, stop codon readthrough was comparably lower in wild type
268 and *sur2*Δ cells treated with 0.1mM GuHCl and 1mM GuHCl demonstrating that we could
269 quantitatively measure the strength of stop codon readthrough in these experiments (Figure
270 2A). Altogether, these data establish that compartmentalization of endo-membranes by a
271 diffusion barrier at the bud neck does not control the inheritance of Sup35 prion seeds during
272 cell division.

**Figure 2**

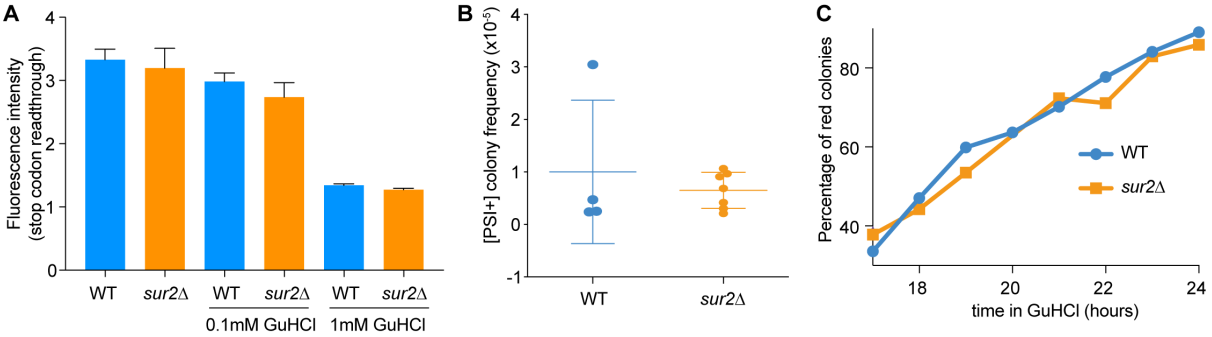


**Figure 2. Endoplasmic reticulum compartmentalization by a lateral membrane diffusion barrier is not required for prion induction and curing.** (A) Fluorescence intensity measured by flow cytometer of [PSI+] WT and [PSI+] *sur2*Δ cells treated or not with 0.1mM and 1mM GuHCl. (B) Frequency of *de novo* [PSI+] appearance and (C) percentage of cells cured of [PSI+] over time. Graphs A and B display mean ± SD.

273

274 *Whi3 super-assemblies and Sup35 foci differ in their association to ER membranes.*

275 Because diffusion barriers affect Whi3 transformation into a prion and not [*PSI*+], we wondered
276 if Sup35 and Whi3 associated to different extends with ER membranes. We first analyzed how
277 Sup35-GFP, in its [*PSI*+] prion form, localized relative to the ER visualized using the

278 translocon subunit Sec61 tagged with mCherry as a marker. Sup35-GFP formed several small
279 foci in dividing cells and we found that most of these foci were spatially excluded from the
280 Sec61 signal (Figure 3A and B, 53.1 ±10.7% of Sup35-GFP foci were away from the Sec61-
281 mCherry signal). We also noticed that 100% of the cells contained at least one focus away
282 from ER membranes (Figure 3C). This may explain why curing and induction of [*PSI*+] is not
283 affected in *sur2*Δ mutant cells. Next, we analyzed the localization of Whi3-mNeonGreen
284 (Whi3-mNG) in its mnemon form relative to Sec61-mCherry. Contrarily to Sup35-GFP, in cells
285 that were exposed to pheromone for 3 hours Whi3-mNG super-assemblies were mostly
286 apposed to ER membranes (72.5 ±4.1% of super-assemblies, Figure 3D and E). Moreover,
287 the fraction apposed to the ER system increased upon longer times of pheromone exposure
288 (82.7 ±2.1% after 4 hours, 90.0 ±3.5% after 6 hours and 92.1 ±3.2% after 10.5 hours, Figure
289 3D and E). Remarkably, while 41.2 ±9.1% of the cells had at least one Whi3-3GFP super-

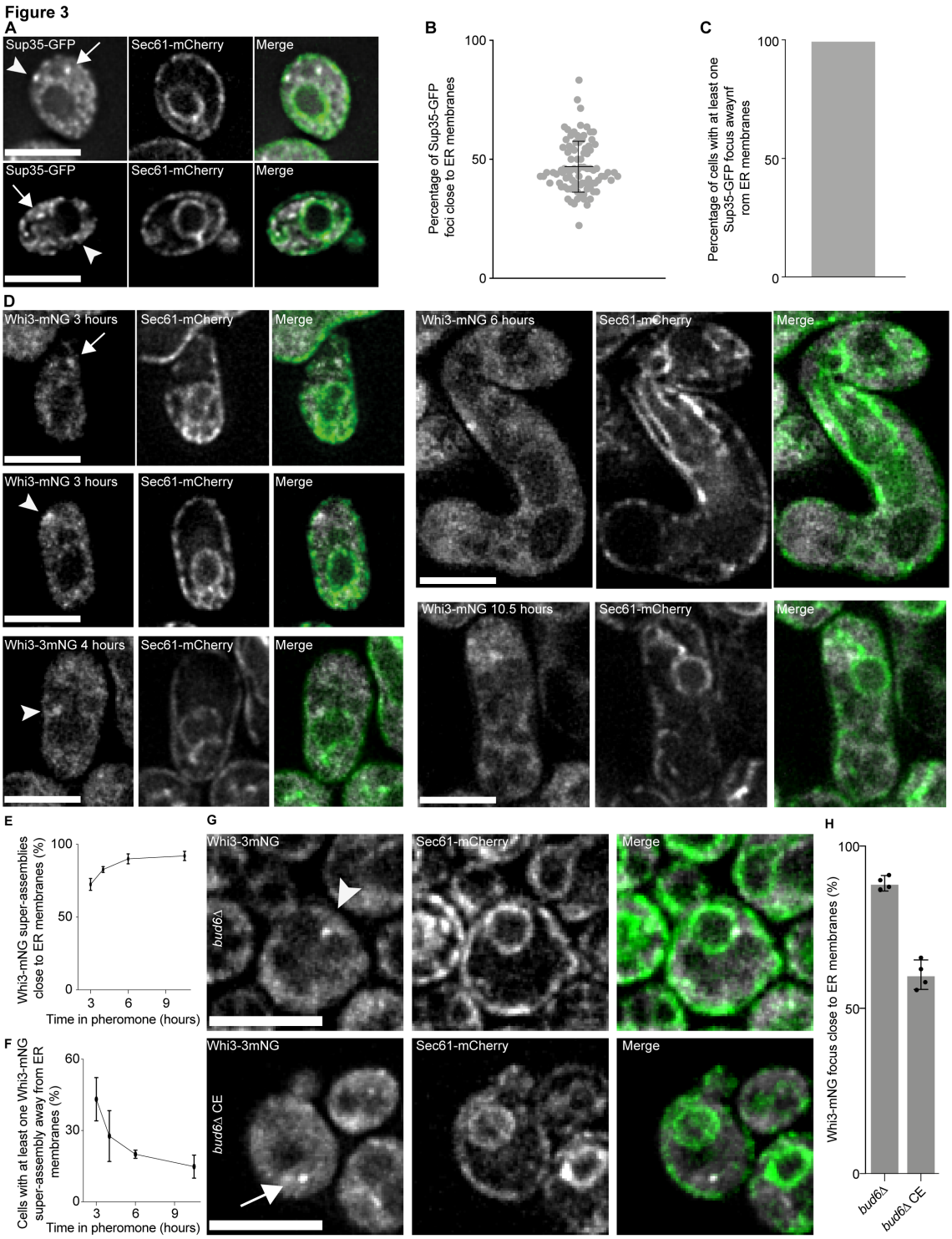


**Figure 3. Sup35 and Whi3 prion foci are not closely linked to ER membranes while Whi3 super-assemblies and granules are.** (A) Single focal plane images of [*PSI+*] cells expressing Sup35-GFP and Sec61-mCherry. (B) Percentage of Sup35 foci close to ER membranes (1180 foci analysed from 90 cells of three independent clones, mean ±SD is presented). (C) Percentage of cells with at least one Sup35-GFP focus away from ER membranes (3 clones with more than 90 cells each). (D) Single focal plane images of cells expressing Whi3-mNG and Sec61-mCherry exposed to pheromone for 3 hours (top left and middle left) and 4 hours (bottom left), and cells exposed for 5 hours to pheromone and released in a pheromone free medium then imaged at 6 hours (top right) and 10.5 hours (bottom right) after initial exposure to pheromone. (E) Percentage of Whi3-mNG super-assemblies close to ER membranes (3 independent clones, >300 super-assemblies from >153 cells were analysed, mean ±SD are presented). (F) Percentage of cells with at least one Whi3-mNG super-assembly away from ER membranes (3 independent clones, >300 super-assemblies from >153 cells were analysed, mean ±SD are presented). (G) Single focal plane images of *bud6*Δ cells (top) and *bud6*Δ CE cells (bottom) expressing Whi3-mNG and Sec61-mCherry. (H) Percentage of Whi3-mNG granules (*bud6*Δ) and foci (*bud6*Δ CE) localizing close to ER membranes (4 clones or isolates, 527 granules and 359 foci in 200 cells were analysed, mean ±SD are presented). For all panel, arrows point at foci away from the ER and arrowheads point at foci close to the ER. Scale bars = 5 µm.

assembly away from the ER after 3 hours of pheromone treatment, this value dropped to 27.7

291 ±10.7%, 20.0 ±1.7% and 14.8 ±4.9% after 4 hours, 6 hours and 10.5 hours of pheromone
292 treatment respectively (Figure 3F). Finally, we analyzed the localization of Whi3-mNG relative
293 to ER membranes in small *bud6*Δ$^{CE}$. We found that 60.27% of the Whi3-mNG foci were close
294 to ER membranes in *bud6*Δ$^{CE}$ cells, in stark contrast to the granules in non-CE *bud6*Δ cells
295 which were much more strongly associated to ER membranes (88.17%, Figure 3G and H).

296 Altogether, we conclude that association of Whi3$^{mnem}$ with ER membranes is tighter with time
297 after escape form pheromone arrest and that a major difference between Whi3$^{mnem}$ super-
298 assemblies and the prion form of Sup35 or the Whi3 foci in CE is their different link to the ER
299 membranes network.

300 *Endoplasmic reticulum compartmentalization is required for the retention of Whi3$^{mnem}$ and the*
301 *pheromone refractory state in the mother cell*

302 The establishment and the maintenance of the pheromone refractory state is facilitated by
303 Whi3's conformational change and super-assembly formation. We wondered whether mother
304 cells with defective diffusion barriers were more likely to pass Whi3 super-assemblies to their
305 daughters. Therefore, we treated cells expressing *WHI3* fused to 3 superfolding Green
306 Fluorescent Proteins in tandem (Whi3-3GFP) with pheromone for 5 hours and then released
307 them in a pheromone free medium for 1.5 hours to allow mother cells to produce a bud. The
308 mother and bud pairs were imaged and the localization of Whi3-3GFP analyzed. Most wild
309 type mother cells contained a super-assembly of Whi3$^{mnem,}$ and we observed similar results in
310 *bud6*Δ*, sur2*Δ and *bud1*Δ mutant cells. However, while only 24.00 ±6.22% of the wild type
311 buds had a super-assembly, 62.24 ±3.85% of the *bud6*Δ*,* 64.01 ±3.65% of the *sur2*Δ and 65.26
312 ±4.15% of the *bud1*Δ mutant buds already had at least one (Figure 4A-B). These data are
313 consistent with a role for diffusion barriers in the retention of Whi3$^{mnem}$ super-assemblies in
314 the mother cells that escaped pheromone arrest.

**Figure 4**

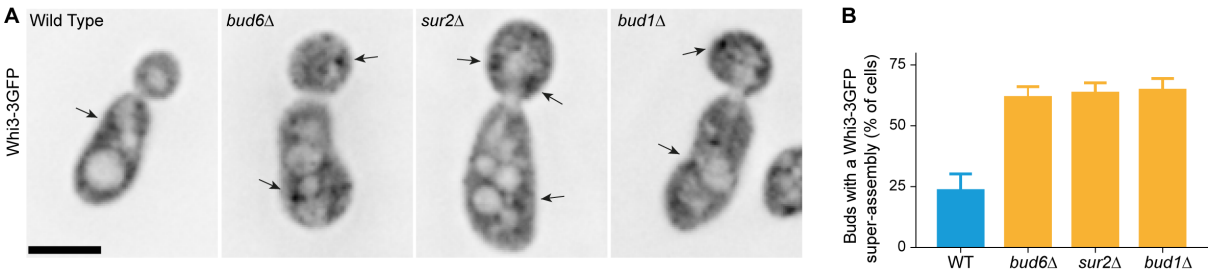


**Figure 4. Whi3-3GFP super-assemblies form in the buds of mutants with a weak diffusion barrier.** (A) Single focal plane images of Whi3-3GFP expressing cells. Scale bar = 5µm. (B) Quantification of buds with a detectable Whi3-3GFP super-assembly (n=122 cells, 148 cells, 180 cells and 165 cells for wild-type, *bud6*Δ, *sur2*Δ and *bud1*Δ cells respectively). Results from *bud6*Δ*, sur2*Δ and *bud1*Δ are significantly different from wild type (p<0.0001, one-way ANOVA).

315 We then tested whether diffusion barriers are required for the retention of the pheromone
316 refractory state in the mother cell. We exposed haploid *MAT***a** cells to pheromone as before

317 (Caudron and Barral, 2013). Wild type cells initially all shmooed upon 7 nM α-factor treatment
318 and 90.5% of the cells escaped pheromone arrest with an average timing of 7.35 ± 3.00 hours
319 (Figure 5A-B). Mother cells kept this refractory state faithfully, 100% of the initial mother cells
320 did not produce a second shmoo after escaping pheromone arrest. We previously found that
321 roughly 90% of the daughter cells from mothers that have escaped from pheromone arrest
322 undergo shmooing in response to pheromone, upon separation from their mother in the
323 presence of pheromone (Caudron and Barral, 2013). We refined our analysis here by
324 separating data depending on whether daughters were the first or subsequent daughters after
325 escape from pheromone arrest. We observed that nearly 50% of the first daughter cells fail to
326 respond to pheromone after birth, while this number drops to 14.2%,13.3%, 6.9% and 4.4%
327 for the subsequent $2^{nd}$, $3^{rd}$, $4^{th}$ and $5^{th}$ daughters of the same mother cell (Figure 5C). In order
328 to assess whether the retention of the pheromone refractory state in the mother cell is indeed
329 dependent on the presence of diffusion barriers at the bud neck, we tested *sur2*Δ, *bud6*Δ and
330 *bud1*Δ mutant cells. For reasons that remain unknown at this stage, cells with a *sur2*Δ mutation
331 escaped from pheromone arrest slightly earlier than wild type cells (5.9 ± 2.0 hours, Figure 5
332 A-B). Once these mother cells escaped, they maintained the pheromone refractory state as
333 efficiently as wild type cells and did not shmoo again. However, the fraction of *sur2*Δ daughter
334 cells that failed to shmoo after separating from their mother cell was increased 1.51, 2.83 and
335 1.66 folds for the $1^{st}$, $2^{nd}$ and $3^{rd}$ daughters respectively. (Figure 5C). The *bud6*Δ mutant cells
336 responded to pheromone as well as wild type cells and escaped pheromone arrest slightly
337 later than them (Figure 5A-B). As for the *sur2*Δ daughter cells, many *bud6*Δ daughter cells
338 failed to shmoo upon separation from their mother cell (Figure 5C). We obtained similar results
339 with *bud1*Δ mutant cells (Figure 5A-C). These results indicate that the ER diffusion barrier
340 reinforces the confinement of the pheromone refractory state to the mother cell.

341 Next, we wondered whether *bud6*Δ, *sur2*Δ or *bud1*Δ mutations had any effect on the timing of
342 escape in the daughter cells that do shmoo in response to pheromone. We reasoned that
343 these daughter cells may escape faster if they inherit factors promoting escape from their
344 mother cell. However, we did not detect any general effect on the timing of daughter cells
345 escape in these mutants (Figure 5D). We still observed that *sur2*Δ daughter cells escaped
346 faster than wild type, *bud6*Δ and *bud1*Δ cells, as their mothers do.

**Figure 5**

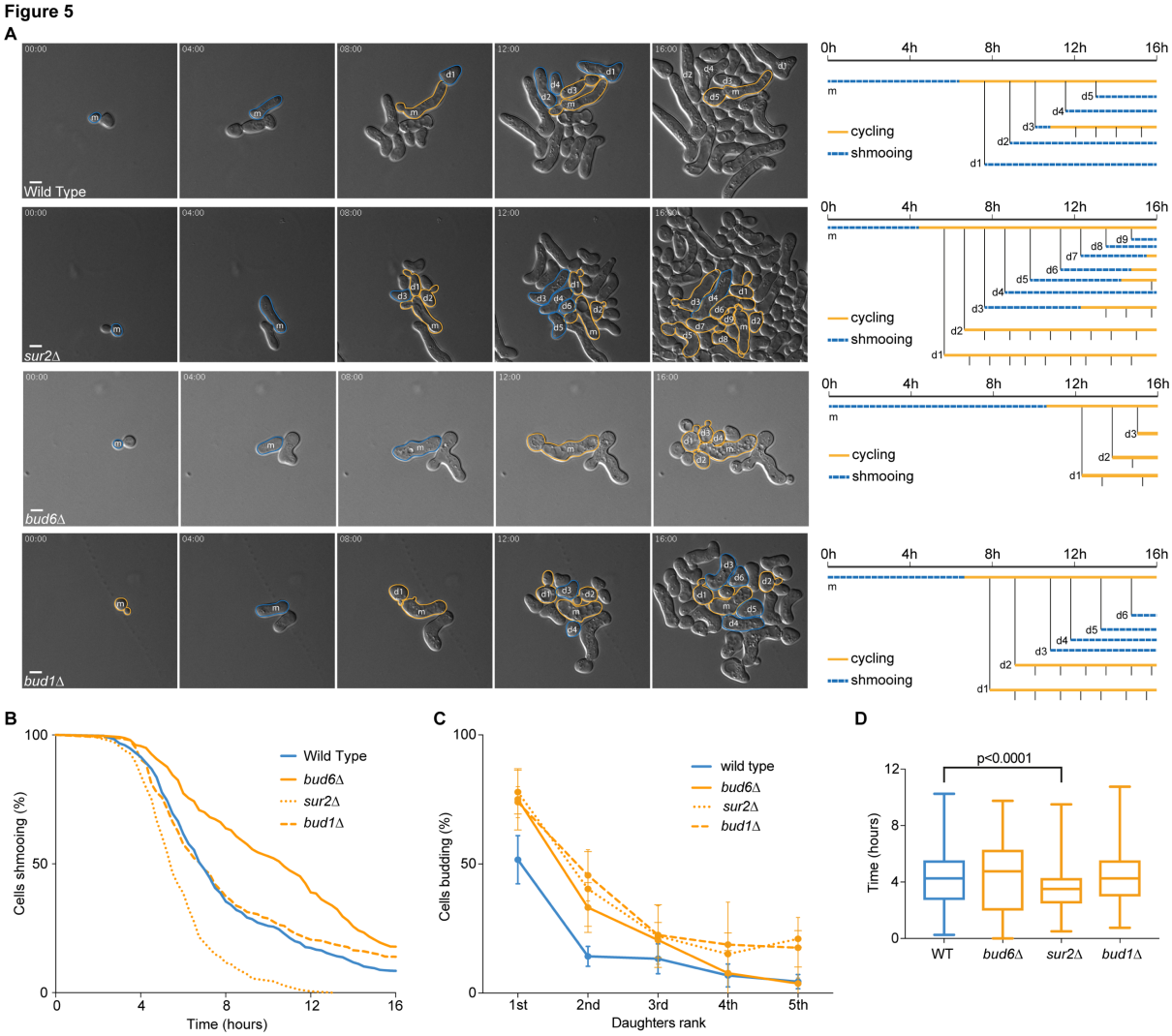


**Figure 5. The ER diffusion barrier prevents daughter cells from inheriting the pheromone refractory state.** (A) Escape of a wild-type, a *bud6*Δ, a *sur2*Δ and a *bud1*Δ cell exposed to 7 nM pheromone. (B) Percentage of initial cells still shmooing after the indicated time (n>154 cells). (C) Percentage of daughter cells budding immediately after separation from the mother cell (n>128 cells, n>121 cells, n>111 cells, n>88 cells and n>59 cells for the 1st, 2nd, 3rd, 4th and 5th daughter respectively). (D) Timing of escape of daughter cells that shmooed (*sur2*Δ is significantly different from wild type, p<0.0001, one-way ANOVA, all other comparisons are not significantly different, n=366 cells, 81 cells, 416 cells and 193 cells for wild-type, *bud6*Δ, *sur2*Δ and *bud1*Δ cells respectively).

347 Altogether, we conclude that diffusion barrier in the cortical ER helps confining the pheromone
348 refractory state to the mother cell. Importantly, in cells lacking a functional barrier the
349 inheritance of the refractory state by the daughter cells does not take place at the cost of the
350 mother cell losing the pheromone refractory state. Indeed, *bud6*Δ, *sur2*Δ and *bud1*Δ mutant
351 mother cells maintained this state as efficiently as wild type cells. Together these results

352 indicate that the ER diffusion barrier confines the pheromone refractory state to the mother
353 cell by preventing the formation of super-assemblies in daughter cells. Strikingly, this role of
354 the barrier is most evident in the first few cycles after pheromone escape by the mother cell
355 and much less so later on.

356

357 *The prion-like domain of Whi3 is required for symmetric inheritance of the refractory state in*
358 *cells with an impaired diffusion barrier.*

359 We next reasoned that if inheritance of the pheromone refractory state by daughter cells
360 depends on Whi3$^{mnem}$ super-assemblies, then preventing the conversion of Whi3 to its
361 mnemon form may lead to less daughter cells inheriting the pheromone refractory state upon
362 diffusion barrier defects. To test this idea, we exposed *whi3-ΔpQ, whi3-ΔpQ bud6Δ* and *whi3-*
363 *ΔpQ bud1Δ* mutant cells to pheromone and analyzed whether the daughters of cells escaping
364 pheromone arrest were shmooing or budding after birth. Most *whi3-ΔpQ* daughter cells
365 shmooed upon birth (Figure 6) and this was not significantly different in *whi3Δ-pQ bud6Δ* and
366 *whi3Δ-pQ bud1Δ* cells. Taken together, these data argue that the Q-rich prion-like domain of
367 Whi3 is involved in the inheritance of the pheromone refractory state by the daughters of cells
368 that lack a diffusion barrier.

369 **Figure 6**

370
371
372
373

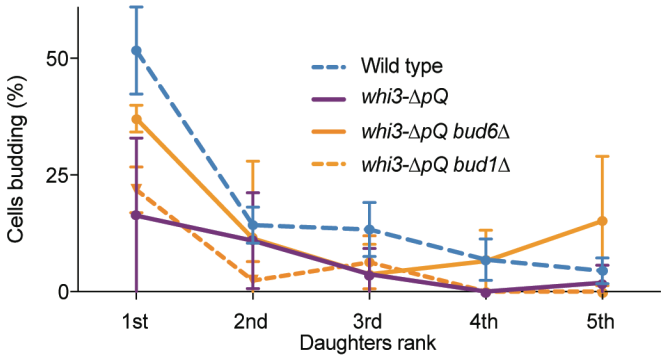


**Figure 6. The polyQ domain of Whi3 is required for inheritance of the pheromone refractory state by diffusion barrier impaired daughter cells.** Percentage of daughter cells of indicated genotypes budding immediately after separation from the mother cell. Mean ±SD are presented.

374

375 **Discussion**

376 In this work, we investigated the mechanisms that allow the pheromone refractory state to be
377 stable in the mother cells over many divisions while preventing it to being passed on to
378 daughter cells. Our data support a model in which Whi3 adopts a self-templating conformation
379 that depends on its prion-like domains upon prolonged pheromone exposure. The self-

380 templating Whi3$^{mnem}$ is confined by diffusion barriers to the mother cell and when this
381 confinement is lost, Whi3$^{mnem}$ does propagate to daughter cells. In a substantial fraction of the
382 cases, it even starts to propagate in a mitotically stable manner, similarly to prions.

383 Indeed, we found that yeast cells can acquire a mitotically stable refractory state to pheromone
384 that we termed constitutive escapers. Some of these CE are small cell sized, phenocopying a
385 loss of function of Whi3. In these small cell sized CE Whi3 forms foci, a hallmark of prion
386 localization in yeast. Moreover, CE induction requires the prion-like domains of Whi3. These
387 data indicate that Whi3 is in a dominant inactive, self-templating prion form in these CE
388 variants. The fact that deleting *WHI3* increases CE frequency indicates that an important step
389 of the transition to the CE state is the inactivation of Whi3 through its conversion to a prion
390 form. Interestingly, the result that *whi3*Δ mutant cells are still able to acquire the CE state
391 indicates the existence of additional prion-like factors in CE cells. Therefore, CE is a promising
392 case for identifying novel prions in yeast.

393 During escape from pheromone arrest in diffusion barrier deficient cells, inheritance of the
394 pheromone refractory state by daughter cells requires the prion like domains of Whi3, also
395 indicating that Whi3$^{mnem}$ is in a self-templating conformation. In diffusion barrier deficient cells,
396 the pheromone refractory state is stable in the mother cells, suggesting that small assemblies
397 are diffusing to daughter cells and seeding the pheromone refractory state there. However, in
398 diffusion barrier defective cells only the first two to three daughter cells can inherit the
399 pheromone refractory state efficiently. This is much less frequent in the next daughter cells.
400 We propose that within the time of two to three cell cycles the super-assemblies mature to a
401 more solid form that no longer generate seeds or captures them efficiently. These data provide
402 experimental support for a mechanism of memory maintenance through a self-templating
403 mechanism. This is a particularly interesting mechanism because it can establish a stable
404 memory that lasts longer than the turnover of the Whi3 protein itself and prevents newly
405 synthesized Whi3 to restore *WHI3* function.

406 All these data argue that Whi3 is able to form several types of assemblies, either being in a
407 mnemon or in a prion form. Since, CE can have different cell sizes, it could also be that Whi3
408 can adopt several types of prion forms, which is reminiscent of the different strains prions can
409 form (Derkatch et al., 1996). It may also be that the mnemon and the prion forms are actually
410 the same and that what is lost are the mechanisms of confinement to the mother cell. CE were
411 frequent in cells with defective diffusion barriers. Because *bud1*Δ cells display this feature, our
412 results point to the ER diffusion barrier playing an important role in the prevention of CE
413 induction. Indeed, only the ER diffusion barrier is affected by *BUD1* deletion, while the nuclear

414 diffusion barrier remains intact. Yet, these observations beg the question of how diffusion
415 barriers could prevent the induction of CE?

416 We found that [*PSI*+] prion induction and curing is not affected by whether the diffusion barriers
417 are present or not. On the contrary, we observed that Whi3$^{mnem}$ super-assemblies and the
418 pheromone refractory state they encode are not confined as efficiently to the mother cell in
419 diffusion barrier defective cells than in wild-type cells. Thus, we propose that one function of
420 the diffusion barriers is to retain Whi3$^{mnem}$ super-assemblies in the compartment where they
421 are formed. Even though Whi3 is not known to be lipidated or having transmembrane domains,
422 Whi3 associates with ER membranes (Vergés et al., 2007). Regardless of how it does so,
423 such an association would allow the diffusion barrier to limit the diffusion of Whi3 seeds along
424 ER membranes through the bud neck. More importantly, we found that Whi3$^{mnem}$ super-
425 assemblies are closely colocalizing with ER membranes during prolonged pheromone
426 response. It will be therefore important in the future to understand how Whi3 is anchored at
427 ER membranes to be able to test our model of retention by the ER diffusion barrier more
428 thoroughly. Altogether a feature of mnemons may be their tight association with ER
429 membranes allowing confinement to one cellular compartment. This is strikingly different to
430 the Sup35 prion, most of which is detected in foci that are away from ER membranes. In this
431 case, the presence of diffusion barriers in the ER membrane has no impact on exchange of
432 seeds across the bud neck. Once Sup35 acquires its prion form in a cell, it can freely invade
433 the bud and maintain the phenotypes associated with it in the progeny, and hence, the whole
434 colony formed. We observed a similar localization pattern respective with ER membranes for
435 Whi3 foci in CE cells. This suggests to us that the Whi3 prion form may differ from the mnemon
436 form at least in part through their membrane association status. Whether the detachment of
437 Whi3 in CE from ER membranes stems from a conformational change inhibiting Whi3
438 interaction with its ER anchor or from a change in the regulation of this interaction will need to
439 be clarified.

440 Altogether, we propose that the absence of the barrier allows for the selection of stable prion
441 strains of Whi3 and possibly other prions. The emergence of these prions would not be able
442 to emerge if they are confined.

443 Many proteins can adopt prion-like behavior across all kingdom of life. Recent effort to
444 characterize these proteins have suggested that this is probably more widespread than
445 anticipated. We presented here that yeast cells have evolved mechanisms to confine and thus
446 control some of them. We propose that this is not restricted to budding yeast. A case could be
447 made for the protein CPEB, which adopt a prion-like conformation at activated dendritic spines
448 (Khan et al., 2015; Si et al., 2010). Interestingly, dendritic spines are highly compartmentalized

449 cellular appendages, and similarly to dividing yeast cells, their compartmentalization and
450 morphology is controlled by septin proteins at the spine neck (Ewers et al., 2014). It may
451 therefore be that CPEB prion conversion is confined to an activated dendritic spine through
452 its compartmentalization by diffusion barriers, which could prevent the spreading of the prion
453 form to the neighbouring non-activated spines. Another consideration may also be that
454 confinement of prion-like elements such as mnemons may prevent their transformation into
455 infectious prion particles. In this case, we could envision that pathologies involving prion-like
456 behaviors may arise when confinement of these elements is lost.

457

458 **Material and Methods**

459 **Strains**

460 Strains used for escape from pheromone arrest were derivatives of the s288c BY4743 wild
461 type (yYB4508: *MAT***a**, *his3Δ1 leu2Δ0, ura3Δ0 met15Δ0 lys2Δ0 ADE2 TRP1 bar1::kanMX*)
462 with deletions obtained according to (Janke et al., 2004) (yYB4507: *sur2::NAT*; yYB4510:
463 *bud6::NAT*; yYB4511: *bud1::NAT*). Strains used for Whi3 localization were derivatives of the
464 wild type (yYB6520: *MAT***a** *ura3Δ0, hisΔ13, leu2Δ0, TRP1, LYS2, ADE2, met15Δ0, WHI3-*
465 *3GFP:kanMX, bar1::HIS3*) backcrossed in yYB4510 for *bud6Δ* (yYB10190), in yYB4507 for
466 *sur2Δ* (yYB10192) or in yYB4511 for *bud1Δ* (yYB10187) strains. Strains for the co-localization
467 of Whi3-3GFP and Sec61-mCherry were obtained by PCR tagging of Sec61 in yYB6520
468 (yFC203: *MAT***a** *ura3Δ0, hisΔ13, leu2Δ0, TRP1, LYS2, ADE2, met15Δ0, WHI3-3GFP:kanMX,*
469 *bar1::HIS3, Sec61-mCherry:kanMX).* W303 strains used to test for [PSI+] induction and curing
470 were obtained from Jonathan Weissman, yYB8040 (*MATα*, *leu2-3,-112; his3-11,-15; trp1-1;*
471 *ura3-1; ade1-14; can1-100,* [*RNQ*+], [*PSI*+]). The *sur2Δ* strain was obtained by deleting *SUR2*
472 according to Janke et al. (Janke et al., 2004) (yYB8435 *MATα*, *leu2-3,-112; his3-11,-15; trp1-*
473 *1; ura3-1; ade1-14; can1-100, sur2::HIS3,* [*RNQ*+], [*PSI*+]). Localisation of Whi3 in *sur2Δ*$^{CE}$
474 was analysed in strain yYB5147 (*his3Δ1, leu2Δ0, met15Δ0, ura3Δ0, LYS2, bar1::kanMX,*
475 *sur2::NatMX, Whi3-GFP:HIS3MX6*). To analyse co-localisation of Sup35-GFP and Sec61-
476 mCherry we used strain yFC202 (*MAT***a/alpha** *SUP35/SUP35-GFP:HIS3; leu2-3,-*
477 *112/leu2Δ0; his3-11,-15/his3Δ1; trp1-1/TRP1; ura3-1/ura3Δ0; ade1-4/ADE1; can1-100/CAN1,*
478 *MET15/met15Δ0, SEC61/Sec61:mCherry:URA3* [*RNQ*+], [*PSI*+]). For stop codon
479 readthrough, we used wild type (*MAT***alpha**, *leu2-3-112, his3-11,-15, trp1-1, ura3-1, ade1-4,*
480 *can1-100,* [*RNQ*+], [*PSI*+], *pRS304 pGPD GST-UGA-GFP-pest:URA3*) or *sur2Δ* strain
481 (*MAT***alpha**, *leu2-3-112, his3-11,-15, trp1-1, ura3-1, ade1-4, can1-100,* [*RNQ*+], [*PSI*+],
482 *pRS304 pGPD GST-UGA-GFP-pest:URA3 sur2::KanMX*).

483

484 **Microscopy**

485 All images were acquired either on a Personal Deltavision (Applied Precision) equipped with
486 a CCD HQ2 camera (Roper) and 250W Xenon lamps controlled by Softworx or a Deltavision
487 Elite (GE Healthcare) equipped with a sCMOS camera and solid-state light-emitting diodes
488 controlled by Softworx. Fluorescein isothiocyanate and tetramethylrhodamine isothiocyanate
489 filters were used for imaging GFP and mCherry fluorescence. Deconvolution was performed
490 using Softworx.

491 **Microfluidics**

492 Experiments were carried out with the ONIX microfluidic perfusion platform with Y04C
493 microfluidic plates (CellAsic). Medium was yeast extract peptone dextrose (YPD)
494 supplemented with 20 mg/ml casein and containing 7 nM α-factor (Figure 2 and 3E) or 6 nM
495 α-factor (Figure 3C-D).

496 **Quantification of Shmooing**

497 Shmooing or budding states were inspected visually. During microfluidic experiments, images
498 were taken every 15 min. Unbudded cells that showed a polarized growth were counted as
499 shmooing. Unbudded cells undergoing isotropic growth were counted as G1 cells. Usually
500 these cells soon started forming a bud. Samples consisted of three independent clones.

501 **Quantification of Whi3-3GFP Super-Assemblies**

502 Cells were grown in YPD supplemented with 20 mg/ml casein and containing 7 nM α-factor
503 and were briefly centrifuged at 600 g, resuspended in SD-TRP medium, placed between slide
504 and coverslip, and imaged immediately. Images were analyzed after deconvolution with
505 Softworx software as before [27]. Three clones with total n > 122 cells were observed for each
506 strain.

507 **Quantification of [PSI+] *de novo* appearance**

508 [PSI+] [PIN+] wild type and *sur2*Δ cells were first cured with 3 passages on YPD agar medium
509 containing 3 mM GuHCl. Red single colonies [psi-] [pin-] were assessed for their ability to
510 become white again. Cells were plated on SC-Ade and YPD and the frequencies of
511 appearance of white colonies were measured. White colonies were tested for their ability to
512 become red again after passages on YPD containing 3 mM GuHCl.

513 **Quantification of [PSI+] curing during treatment with GuHCl**

514 Cells were grown overnight in liquid YPD and diluted in the morning to $OD_{600nm}$ = 0.2 in YPD
515 with 3 mM GuHCl. Samples were taken every 30 minutes and plated on synthetic medium
516 with low adenine concentration. Liquid cultures were kept in exponential phase during the
517 experiment. Colonies were allowed to grow at 30ºC for several days and the proportion of
518 white and red colonies was assessed after 2 days of incubation at 4ºC to allow for the red
519 colour to develop well. We initially determined that curing started to happen after 12 hours of
520 GuHCl treatment for both wild type and *sur2*Δ strains.

521

522 **Quantification of Stop-codon read-through by flow cytometry**

523 For the stop codon read through experiments, wild-type [*PSI*+] and *sur2*Δ [*PSI*+] cells
524 expressing chromosomally integrated pGPD GST-UGA-GFP-pest were grown for 5 hours
525 without GuHCl or with 0.1mM or 1mM GuHCl. The GFP fluorescence intensity was measured
526 with a BD Accuri C6 Flow Cytometer using 488 nm laser and 533/30 BD filter for 100 000
527 cells/ clone (3 clones each). The data was analyzed using FlowJo software (FlowJo LLC).

528 **Quantification of CE frequencies**

529 Diploid strains heterozygous for the different mutations were sporulated (for example
530 *SUR2/sur2*Δ or *WHI3/whi3*Δ). *MAT***a** spores were selected and their genotypes determined by
531 growth on selection media. Strains were grown in YPD until mid-log phase and spotted on
532 solid YPD and solid YPD containing 0.6μM α-factor. Colonies were counted after 2-3 days of
533 growth at 30ºC.

534 **Cell sizes measurements**

535 Cell sizes were determined using a CASY cell counter model TTC (Schärfe system). Strains
536 were grown to early log phase, diluted in CASYton (Electrolyte buffer from Schärfe system)
537 and processed according to the manufacturer instructions.

538 **Quantification of Sup35 foci and Whi3 super-assemblies/foci/granules co-localisation**
539 **with ER membranes**

540 For Whi3-3GFP localisation, cells were grown in YPD supplemented with 20 mg/ml casein
541 and containing 7nM α-factor and were briefly centrifuged at 600 g, resuspended in SD-TRP
542 medium, placed on a SC-TRP agar pad covered by a coverslip, and imaged immediately.
543 Images were analysed after deconvolution with Softworx software. Three clones with total n =
544 194 cells, 250 cells, 170 cells and 153 cells for 3 hours, 4 hours, 6 hours and 10.5 hours
545 condition were observed for each strain. A total of 333, 402, 393 and 317 super-assemblies

546 were analysed at 3 hours, 4 hours, 6 hours and 10.5 hours' time points. Note that we only
547 analysed super-assemblies that were in the 5 best focal planes as co-localisation was difficult
548 to assess on the top and bottom focal planes and we only counted Sup35-GFP foci and Whi3-
549 3GFP super-assemblies in the mother cells.

550 **Acknowledgements**

551 We would like to thank Robin Hannay for his help in creating some of the strains. This work
552 was supported by a Biotechnology and Biological Sciences Research Council Project grant
553 (BB/S001204/1) to FC, QMUL to FC and YL, the Academy of Finland (317038) and Sigrid
554 Jusélius Foundation to JS and the European Research Council (BarrAge 250278) and ETH
555 Zurich (to J.S., F.C. and Y.B.).

556

557 **References**

558 Alberti S, Halfmann R, King O, Kapila A, Lindquist S. 2009. A systematic survey identifies
559 prions and illuminates sequence features of prionogenic proteins. *Cell* **137**:146–158.
560 doi:10.1016/j.cell.2009.02.044
561 Bender A, Pringle JR. 1989. Multicopy suppression of the cdc24 budding defect in yeast by
562 CDC42 and three newly identified genes including the ras-related gene RSR1. *Proc*
563 *Natl Acad Sci U S A* **86**:9976–9980.
564 Brown JCS, Lindquist S. 2009. A heritable switch in carbon source utilization driven by an
565 unusual yeast prion. *Genes Dev* **23**:2320–2332. doi:10.1101/gad.1839109
566 Caudron F, Barral Y. 2013. A super-assembly of Whi3 encodes memory of deceptive
567 encounters by single cells during yeast courtship. *Cell* **155**:1244–1257.
568 doi:10.1016/j.cell.2013.10.046
569 Caudron F, Barral Y. 2009. Septins and the lateral compartmentalization of eukaryotic
570 membranes. *Dev Cell* **16**:493–506. doi:10.1016/j.devcel.2009.04.003
571 Clay L, Caudron F, Denoth-Lippuner A, Boettcher B, Buvelot Frei S, Snapp EL, Barral Y. 2014.
572 A sphingolipid-dependent diffusion barrier confines ER stress to the yeast mother
573 cell. *eLife* **3**:e01883. doi:10.7554/eLife.01883
574 Coustou V, Deleu C, Saupe S, Begueret J. 1997. The protein product of the het-s
575 heterokaryon incompatibility gene of the fungus Podospora anserina behaves as a
576 prion analog. *Proc Natl Acad Sci* **94**:9773–9778. doi:10.1073/pnas.94.18.9773
577 Denoth-Lippuner A, Krzyzanowski MK, Stober C, Barral Y. 2014. Role of SAGA in the
578 asymmetric segregation of DNA circles during yeast ageing. *eLife* **3**.
579 doi:10.7554/eLife.03790
580 Derdowski A, Sindi SS, Klaips CL, DiSalvo S, Serio TR. 2010. A size threshold limits prion
581 transmission and establishes phenotypic diversity. *Science* **330**:680–683.
582 doi:10.1126/science.1197785
583 Derkatch IL, Chernoff YO, Kushnirov VV, Inge-Vechtomov SG, Liebman SW. 1996. Genesis
584 and variability of [PSI] prion factors in Saccharomyces cerevisiae. *Genetics* **144**:1375–
585 1386.

586 Ewers H, Tada T, Petersen JD, Racz B, Sheng M, Choquet D. 2014. A Septin-Dependent
587 Diffusion Barrier at Dendritic Spine Necks. *PloS One* **9**:e113916.
588 doi:10.1371/journal.pone.0113916
589 Ferreira PC, Ness F, Edwards SR, Cox BS, Tuite MF. 2001. The elimination of the yeast [PSI+]
590 prion by guanidine hydrochloride is the result of Hsp104 inactivation. *Mol Microbiol*
591 **40**:1357–1369.
592 Garì E, Volpe T, Wang H, Gallego C, Futcher B, Aldea M. 2001. Whi3 binds the mRNA of the
593 G1 cyclin CLN3 to modulate cell fate in budding yeast. *Genes Dev* **15**:2803–2808.
594 doi:10.1101/gad.203501
595 Goedert M. 2015. Alzheimer's and Parkinson's diseases: The prion concept in relation to
596 assembled Aβ, tau, and α-synuclein. *Science* **349**:1255555.
597 doi:10.1126/science.1255555
598 Graziano BR, DuPage AG, Michelot A, Breitsprecher D, Moseley JB, Sagot I, Blanchoin L,
599 Goode BL. 2011. Mechanism and cellular function of Bud6 as an actin nucleation-
600 promoting factor. *Mol Biol Cell* **22**:4016–4028. doi:10.1091/mbc.E11-05-0404
601 Graziano BR, Jonasson EM, Pullen JG, Gould CJ, Goode BL. 2013. Ligand-induced activation
602 of a formin-NPF pair leads to collaborative actin nucleation. *J Cell Biol* **201**:595–611.
603 doi:10.1083/jcb.201212059
604 Harvey ZH, Chen Y, Jarosz DF. 2018. Protein-Based Inheritance: Epigenetics beyond the
605 Chromosome. *Mol Cell* **69**:195–202. doi:10.1016/j.molcel.2017.10.030
606 Hou F, Sun L, Zheng H, Skaug B, Jiang Q-X, Chen ZJ. 2011. MAVS forms functional prion-like
607 aggregates to activate and propagate antiviral innate immune response. *Cell*
608 **146**:448–461. doi:10.1016/j.cell.2011.06.041
609 Hu Q, Milenkovic L, Jin H, Scott MP, Nachury MV, Spiliotis ET, Nelson WJ. 2010. A septin
610 diffusion barrier at the base of the primary cilium maintains ciliary membrane
611 protein distribution. *Sci N Y NY* **329**:436–439. doi:10.1126/science.1191054
612 Janke C, Magiera MM, Rathfelder N, Taxis C, Reber S, Maekawa H, Moreno-Borchart A,
613 Doenges G, Schwob E, Schiebel E, Knop M. 2004. A versatile toolbox for PCR-based
614 tagging of yeast genes: new fluorescent proteins, more markers and promoter
615 substitution cassettes. *Yeast Chichester Engl* **21**:947–962. doi:10.1002/yea.1142
616 Jarosz DF, Brown JCS, Walker GA, Datta MS, Ung WL, Lancaster AK, Rotem A, Chang A,
617 Newby GA, Weitz DA, Bisson LF, Lindquist S. 2014. Cross-kingdom chemical
618 communication drives a heritable, mutually beneficial prion-based transformation of
619 metabolism. *Cell* **158**:1083–1093. doi:10.1016/j.cell.2014.07.025
620 Khan MR, Li L, Pérez-Sánchez C, Saraf A, Florens L, Slaughter BD, Unruh JR, Si K. 2015.
621 Amyloidogenic Oligomerization Transforms Drosophila Orb2 from a Translation
622 Repressor to an Activator. *Cell* **163**:1468–1483. doi:10.1016/j.cell.2015.11.020
623 Kim SK, Shindo A, Park TJ, Oh EC, Ghosh S, Gray RS, Lewis RA, Johnson CA, Attie-Bittach T,
624 Katsanis N, Wallingford JB. 2010. Planar cell polarity acts through septins to control
625 collective cell movement and ciliogenesis. *Sci N Y NY* **329**:1337–1340.
626 doi:10.1126/science.1191184
627 Lang GI, Murray AW. 2008. Estimating the per-base-pair mutation rate in the yeast
628 Saccharomyces cerevisiae. *Genetics* **178**:67–82. doi:10.1534/genetics.107.071506
629 Luedeke C, Frei SB, Sbalzarini I, Schwarz H, Spang A, Barral Y. 2005. Septin-dependent
630 compartmentalization of the endoplasmic reticulum during yeast polarized growth. *J*
631 *Cell Biol* **169**:897–908. doi:10.1083/jcb.200412143

632 Moore SA. 1984. Yeast cells recover from mating pheromone alpha factor-induced division
633 arrest by desensitization in the absence of alpha factor destruction. *J Biol Chem*
634 **259**:1004–1010.
635 Mostowy S, Cossart P. 2012. Septins: the fourth component of the cytoskeleton. *Nat Rev*
636 *Mol Cell Biol* **13**:183–194. doi:10.1038/nrm3284
637 Narayanan S, Walter S, Reif B. 2006. Yeast prion-protein, sup35, fibril formation proceeds by
638 addition and substraction of oligomers. *Chembiochem Eur J Chem Biol* **7**:757–765.
639 doi:10.1002/cbic.200500382
640 Prusiner SB. 1982. Novel proteinaceous infectious particles cause scrapie. *Sci N Y NY*
641 **216**:136–144.
642 Saarikangas J, Barral Y. 2011. The emerging functions of septins in metazoans. *EMBO Rep*
643 **12**:1118–1126. doi:10.1038/embor.2011.193
644 Saarikangas J, Caudron F, Prasad R, Moreno DF, Bolognesi A, Aldea M, Barral Y. 2017.
645 Compartmentalization of ER-Bound Chaperone Confines Protein Deposit Formation
646 to the Aging Yeast Cell. *Curr Biol CB* **27**:773–783. doi:10.1016/j.cub.2017.01.069
647 Serio TR, Cashikar AG, Kowal AS, Sawicki GJ, Moslehi JJ, Serpell L, Arnsdorf MF, Lindquist SL.
648 2000. Nucleated Conformational Conversion and the Replication of Conformational
649 Information by a Prion Determinant. *Science* **289**:1317–1321.
650 doi:10.1126/science.289.5483.1317
651 Sharma SV, Agatsuma T, Nakano H. 1998. Targeting of the protein chaperone, HSP90, by the
652 transformation suppressing agent, radicicol. *Oncogene* **16**:2639–2645.
653 doi:10.1038/sj.onc.1201790
654 Shcheprova Z, Baldi S, Frei SB, Gonnet G, Barral Y. 2008. A mechanism for asymmetric
655 segregation of age during yeast budding. *Nature* **454**:728–734.
656 doi:10.1038/nature07212
657 Si K, Choi Y-B, White-Grindley E, Majumdar A, Kandel ER. 2010. Aplysia CPEB can form prion-
658 like multimers in sensory neurons that contribute to long-term facilitation. *Cell*
659 **140**:421–435. doi:10.1016/j.cell.2010.01.008
660 Suzuki G, Shimazu N, Tanaka M. 2012. A Yeast Prion, Mod5, Promotes Acquired Drug
661 Resistance and Cell Survival Under Environmental Stress. *Science* **336**:355–359.
662 doi:10.1126/science.1219491
663 Toure A, Rode B, Hunnicutt GR, Escalier D, Gacon G. 2011. Septins at the annulus of
664 mammalian sperm. *Biol Chem* **392**:799–803. doi:10.1515/BC.2011.074
665 True HL, Lindquist SL. 2000. A yeast prion provides a mechanism for genetic variation and
666 phenotypic diversity. *Nature* **407**:477–483. doi:10.1038/35035005
667 Tuite MF. 2016. Remembering the Past: A New Form of Protein-Based Inheritance. *Cell*
668 **167**:302–303. doi:10.1016/j.cell.2016.09.036
669 Tuite MF, Cox BS. 2006. The [PSI+] prion of yeast: a problem of inheritance. *Methods San*
670 *Diego Calif* **39**:9–22. doi:10.1016/j.ymeth.2006.04.001
671 Tuite MF, Mundy CR, Cox BS. 1981. Agents that cause a high frequency of genetic change
672 from [psi+] to [psi-] in Saccharomyces cerevisiae. *Genetics* **98**:691–711.
673 Vergés E, Garì E, Gallego C, Aldea M. 2007. Cyclin Cln3 is retained at the ER and released by
674 the J chaperone Ydj1 in late G1 to trigger cell cycle entry. **26**:649–662.
675 doi:10.1016/j.molcel.2007.04.023
676 Wickner RB, Shewmaker FP, Bateman DA, Edskes HK, Gorkovskiy A, Dayani Y, Bezsonov EE.
677 2015. Yeast prions: structure, biology, and prion-handling systems. *Microbiol Mol*
678 *Biol Rev MMBR* **79**:1–17. doi:10.1128/MMBR.00041-14

Yuan AH, Hochschild A. 2017. A bacterial global regulator forms a prion. *Sci N Y NY* **355**:198–201. doi:10.1126/science.aai7776